



Received 22 July 2020
Accepted 24 August 2020

Edited by W. T. A. Harrison, University of Aberdeen, Scotland

Keywords: cocrystal structure; zwitterion; oxyresveratrol; resveratrol.

CCDC references: 2024883; 2024882

Supporting information: this article has supporting information at journals.iucr.org/e

Syntheses and crystal structures of hydrated and anhydrous 1:2 cocrystals of oxyresveratrol and zwitterionic proline

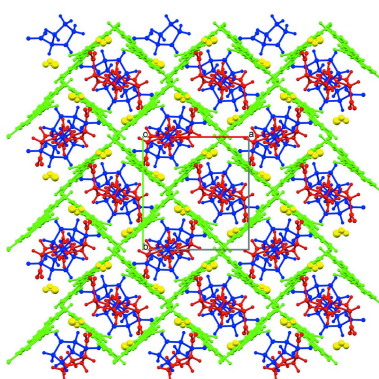
Passaporn Ouiyangkul,^a Saowanit Saithong^{b,c} and Vimon Tantishaiyakul^{a,d*}

^aDepartment of Pharmaceutical Chemistry, Faculty of Pharmaceutical Sciences, Prince of Songkla University, Hat-Yai, 90112, Thailand, ^bDivision of Physical Science and Center of Excellence for Innovation in Chemistry, Faculty of Science, Prince of Songkla University, Hat-Yai, Songkhla, 90112, Thailand, ^cMedical Science Research and Innovation Institute, Research and Development Office, Prince of Songkla University, Hat-Yai, 90112, Thailand, and ^dCenter of Excellence for Drug Delivery System and Department of Pharmaceutical Chemistry, Faculty of Pharmaceutical Sciences, Prince of Songkla University, Hat-Yai, 90112, Thailand. *Correspondence e-mail: vimon.t@psu.ac.th

The hydrated and anhydrous 1:2 cocrystals of oxyresveratrol (*4-[*(*E*)-2-(3,5-dihydroxyphenyl)ethenyl]benzene-1,3-diol; OXY; $C_{14}H_{12}O_4$) and proline [*(S*)-pyrrolidine-2-carboxylic acid; PRO; $C_5H_9NO_2$], namely, *4-[*(*E*)-2-(3,5-dihydroxyphenyl)ethenyl]benzene-1,3-diol bis[*(S*)-pyrrolidin-1-iium-2-carboxylate] monohydrate, $C_{14}H_{12}O_4 \cdot 2C_5H_9NO_2 \cdot H_2O$, and the anhydrous form, $C_{14}H_{12}O_4 \cdot 2C_5H_9NO_2$, were obtained by crystallization at different temperatures. Both of them crystallize with orthorhombic ($P2_12_12_1$) symmetry. The structures display N–H···O and O–H···O hydrogen-bonding interactions between PRO and PRO, OXY and OXY, and OXY and PRO. In the hydrated cocrystal, these types of contacts are also observed between the OXY, PRO and water molecules. A combination of these interactions leads to a three-dimensional supramolecular assembly in each case. Hirshfeld surfaces were used to gain further insight into the intermolecular interactions in the packing, including the relative percentage contributions of the significant intermolecular H···H and H···O/O···H contacts.

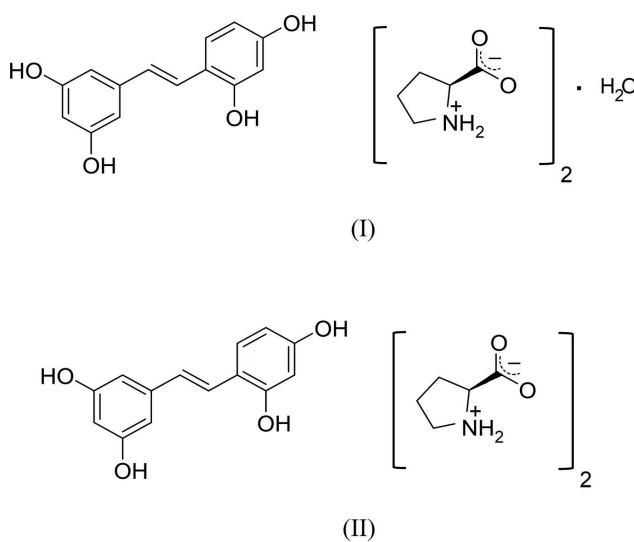
1. Chemical context

Oxyresveratrol (*4-[*(*E*)-2-(3,5-dihydroxyphenyl)ethenyl]-benzene-1,3-diol; OXY; $C_{14}H_{12}O_4$) is a natural stilbenoid found in various plants, such as *Morus alba* L. (Lu *et al.*, 2017). It has several biological activities, including neuroprotective and hepatoprotective effects (Shah *et al.*, 2019; Jia *et al.*, 2018; Chao *et al.*, 2008). As the aqueous solubility of OXY is low, there have been attempts to improve its solubility and oral bioavailability by cocrystallization with citric acid and glutaric acid (Suzuki *et al.*, 2019). Proline [*(S*)-pyrrolidine-2-carboxylic acid; PRO; $C_5H_9NO_2$] is a natural amino acid that has a secondary amino group in the form of a pyrrolydic ring. It is an osmoprotectant and is used frequently in many pharmaceutical and biotechnological applications (Panday, 2011). PRO has been used as a cocrystal former in various drugs and pharmacological active compounds because of its molecular rigidity and high solubility in water (Chesna *et al.*, 2017; Surov *et al.*, 2018; Tilborg *et al.*, 2014). According to previous studies, the phenolic hydroxyl groups of flavonoids are able to form charge-assisted hydrogen bonds with the carboxylate moiety of PRO (He *et al.*, 2016). Moreover, PRO could form a cocrystal with resveratrol [*(E*)-5-(4-hydroxystyryl)benzene-1,3-diol; RES; $C_{14}H_{12}O_3$], which is a close analogue of OXY



OPEN ACCESS

(He *et al.*, 2017). Therefore, PRO is a good candidate as a cocrystal former for cocrystallization with OXY and we now describe the syntheses and structures of hydrated and anhydrous 1:2 cocrystals of OXY and PRO, hereafter (I) and (II).



2. Structural commentary

Both cocrystals of OXY and PRO form a 1:2 stoichiometry in the orthorhombic system, space group $P2_12_12_1$, with $Z = 4$. The asymmetric unit of (I) contains two PRO, one OXY and one water molecule while the asymmetric unit of (II) consists of only two PRO and one OXY molecules, as depicted in Fig. 1. The dihedral angle between the planes of the OXY C1–C6 and C9–C14 phenyl rings in (I) is $7.1(2)^\circ$. This is slightly different from the previous report [$9.39(9)^\circ$] of the corresponding angle in OXY· $2\text{H}_2\text{O}$ (Deng *et al.*, 2012). However, a more twisted dihedral angle between these phenyl rings is observed in (II), of $14.15(19)^\circ$. It might be caused by the influence of hydrogen-bonding interactions in the crystal. In addition, the zwitterionic form of the PRO molecules of both cocrystals is confirmed by the C–O and C–N bond lengths.

Table 1
Hydrogen-bond geometry (\AA , $^\circ$) for (I).

$D-\text{H}\cdots A$	$D-\text{H}$	$\text{H}\cdots A$	$D\cdots A$	$D-\text{H}\cdots A$
O1–H1'…O8	0.84 (2)	1.78 (3)	2.597 (3)	166 (5)
O2–H2'…O6	0.92	1.74	2.647 (3)	172
O3–H3'…O2 ⁱ	0.85 (2)	1.93 (3)	2.778 (3)	175 (5)
O4–H4'…O9	0.99	1.76	2.575 (6)	137
O9–H9A…O7 ⁱⁱ	0.89 (2)	1.76 (3)	2.639 (5)	168 (4)
N1–H1A…O6 ⁱⁱⁱ	0.89	1.90	2.777 (4)	168
N1–H1B…O4 ^{iv}	0.89	2.28	2.951 (4)	132
N1–H1B…O9 ^{iv}	0.89	2.47	3.105 (5)	129
N2–H2A…O8 ^v	0.89	1.90	2.753 (3)	159
N2–H2B…O5 ^{vi}	0.89	2.07	2.829 (3)	143
N2–H2B…O7	0.89	2.24	2.677 (4)	110
C6–H6…O6	0.93	2.58	3.261 (4)	130

Symmetry codes: (i) $-x, y + \frac{1}{2}, -z + \frac{1}{2}$; (ii) $x + \frac{1}{2}, -y + \frac{3}{2}, -z + 1$; (iii) $x + \frac{1}{2}, -y + \frac{1}{2}, -z + 1$; (iv) $-x + 1, y - \frac{1}{2}, -z + \frac{1}{2}$; (v) $-x, y - \frac{1}{2}, -z + \frac{3}{2}$; (vi) $-x + \frac{1}{2}, -y + 1, z + \frac{1}{2}$.

3. Supramolecular features

The packing for (I) and (II) is shown in Fig. 2. The two PRO molecules (PRO 1 and PRO 2) are indicated in blue and red, respectively, whereas the OXY and water molecules are shown in green and yellow, respectively. The main architectures of (I) and (II) are quite similar but there are clearly differences regarding the water molecule in (I).

The PRO 1 and PRO 2 molecules form a three-dimensional network of N–H…O hydrogen bonds between the H atoms of NH₂ groups and O atoms of carboxylate groups: N1–H1A…O6ⁱⁱⁱ, N2–H2A…O8^v and N2–H2B…O5^{vi} for (I) and N1–H1B…O5ⁱⁱⁱ, N1–H1A…O8^{iv} and N2–H2B…O6^{vi} for (II) (see Tables 1 and 2, where the symmetry codes are defined). The hydrogen-bonding interactions between PRO 1 and PRO 2 of both cocrystals viewed down [100] are shown in Fig. 3. The phenolic hydroxyl groups from the OXY molecule interact with O atoms of the carboxylate groups of the PRO

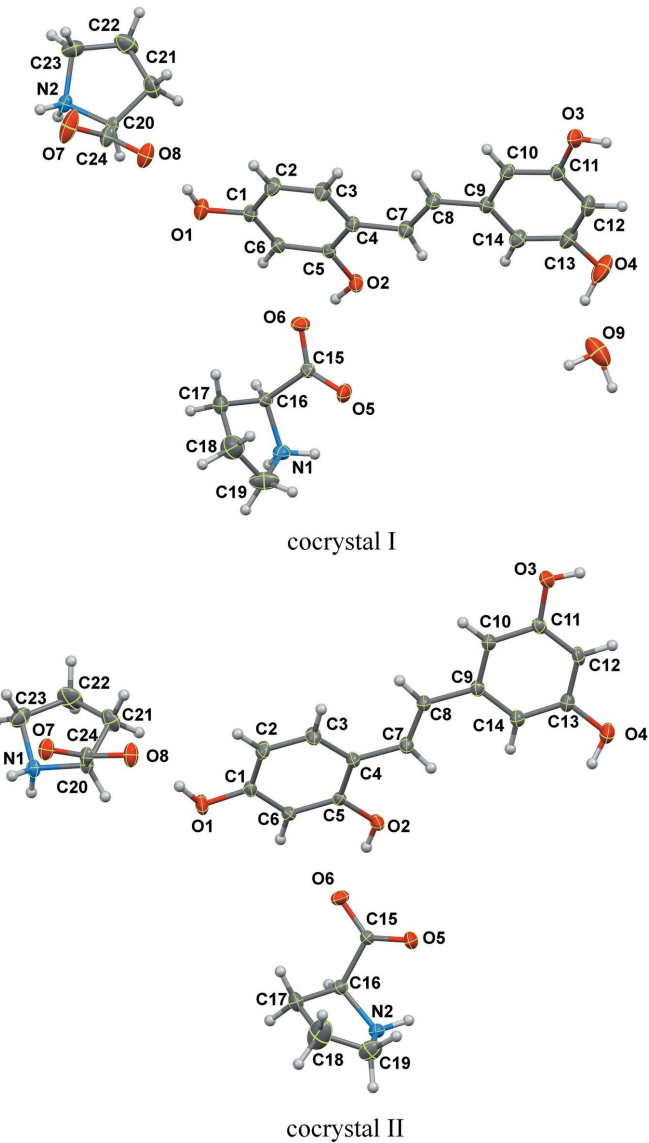


Figure 1

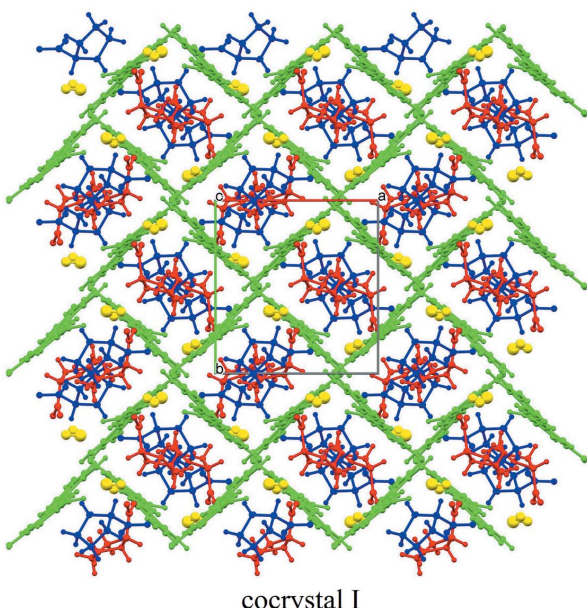
The molecular structures of (I) and (II) showing 50% displacement ellipsoids.

molecules *via* O—H···O hydrogen bonds, namely O2—H2'···O6 and O1—H1'···O8 for (I) and O1—H1'···O8, O2—H2'···O6 and O4—H4'···O7ⁱⁱ for (II). In addition, one of the four hydroxyl groups of OXY accepts a hydrogen bond N1—H1B···O4^{iv} from PRO at an N···O distance of 2.951 (4) Å in (I) while the equivalent bond in (II) is observed at 2.920 (4) Å for N2—H2A···O4^v. Moreover, hydrogen-bonding contacts among the OXY molecules in both cocrystals are observed between phenolic hydroxyl groups, O3—H3'···O2ⁱ, for both cocrystals. Further hydrogen-bond interactions involving the water molecule are observed in (I): N1—H1B···O9^{iv} between PRO and water [N···O = 3.105 (5) Å] and O4—H4'···O9 [2.575 (6) Å] and O9—H9A···O7ⁱⁱ [2.639 (5) Å] interactions

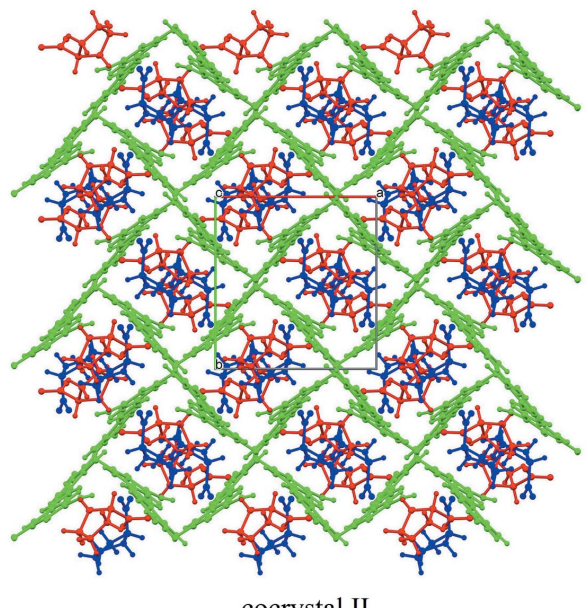
Table 2
Hydrogen-bond geometry (Å, °) for (II).

D—H···A	D—H	H···A	D···A	D—H···A
O1—H1'···O8	0.96	1.70	2.642 (4)	169
O2—H2'···O6	0.82 (2)	1.83 (3)	2.647 (3)	175 (5)
O3—H3'···O2 ⁱ	0.87	1.92	2.784 (3)	171
O4—H4'···O7 ⁱⁱ	0.89 (2)	1.95 (3)	2.794 (4)	159 (4)
N1—H1B···O5 ⁱⁱⁱ	0.89	2.04	2.827 (3)	146
N1—H1A···O8 ^{iv}	0.89	1.90	2.733 (4)	154
N2—H2A···O4 ^v	0.89	2.11	2.920 (4)	150
N2—H2B···O6 ^{vi}	0.89	1.87	2.734 (4)	163
C6—H6···O6	0.93	2.61	3.282 (4)	130

Symmetry codes: (i) $-x, y + \frac{1}{2}, -z + \frac{1}{2}$; (ii) $x + \frac{1}{2}, -y + \frac{3}{2}, -z + 1$; (iii) $-x + \frac{1}{2}, -y + 1, z + \frac{1}{2}$; (iv) $-x, y - \frac{1}{2}, -z + \frac{3}{2}$; (v) $-x + 1, y - \frac{1}{2}, -z + \frac{1}{2}$; (vi) $x + \frac{1}{2}, -y + \frac{1}{2}, -z + 1$.



cocrystal I

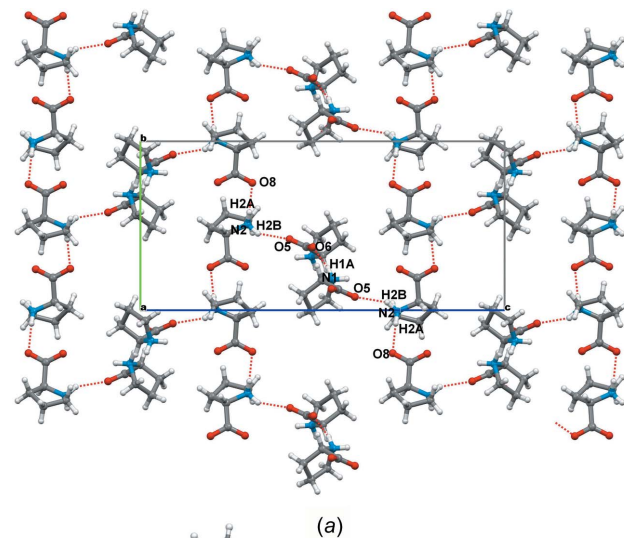


cocrystal II

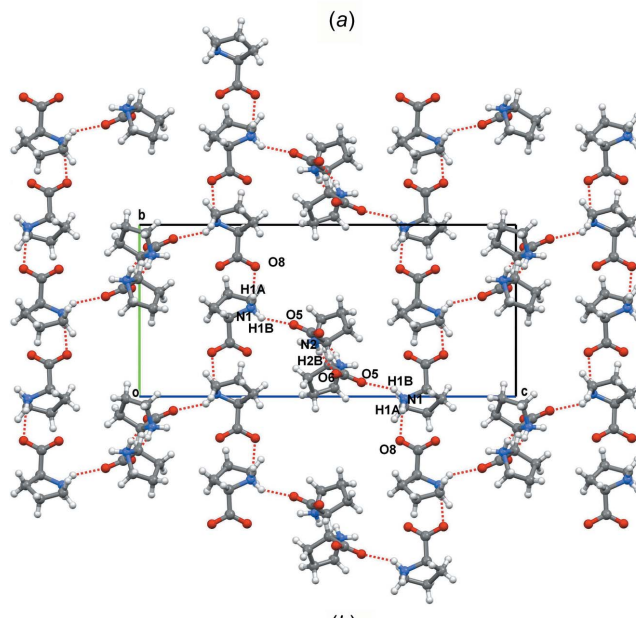
Figure 2

The packing in (I) and (II); colour code PRO 1 (blue), PRO 2 (red), OXY (green) and water (yellow).

between OXY and water molecules. Taken together, the hydrogen bonds in both cocrystals form complex three-dimensional supramolecular architectures.



(a)



(b)

Figure 3

Hydrogen-bond interactions between the PRO molecules viewed down [100] in (a) (I) and (b) (II).

4. Hirshfeld surface analysis

Hirshfeld surface analysis and two dimensional fingerprint plots are used to provide the additional insight of the weak intermolecular contacts and intermolecular interactions in the crystal packing of molecules (McKinnon *et al.*, 2004; 2007; Spackman & Jayatilaka, 2009). The blue, white and red areas in the d_{norm} -mapped Hirshfeld surfaces indicate interatomic contacts longer, equal to and shorter than the sum of the van der Waals radii, respectively. Analysis of (I) and (II) was performed by using *Crystal Explorer* 17.5 (Turner *et al.*, 2017). The Hirshfeld surfaces are plotted for individual components, to examine the interactions of the main molecules (PRO and OXY) in the cocrystals.

The Hirshfeld surfaces around the PRO molecules mapped over d_{norm} are shown in Fig. 4 with selected atoms labelled (compare Tables 1 and 2). There are red spots on the surface close to H atoms of the amine group inside the surface of PRO molecules in both cocrystals, H1A and H1B for PRO 1 and H2A and H2B for PRO 2. The inside zones indicate hydrogen-bond donors to acceptor O atoms at outside surfaces of the nearby carboxylate groups of adjacent PRO molecules (N—H···O type), hydroxyl group of OXY (N—H···O type) and O atoms of water [only for (I), O—H···O and N—H···O forms]. Besides, the O atoms of the carboxylate groups of both PRO molecules acting as hydrogen-bond acceptors interact with the hydrogen-bond donor NH₂ group of PRO molecules on the outside surfaces, as discussed in the *Supramolecular features* section.

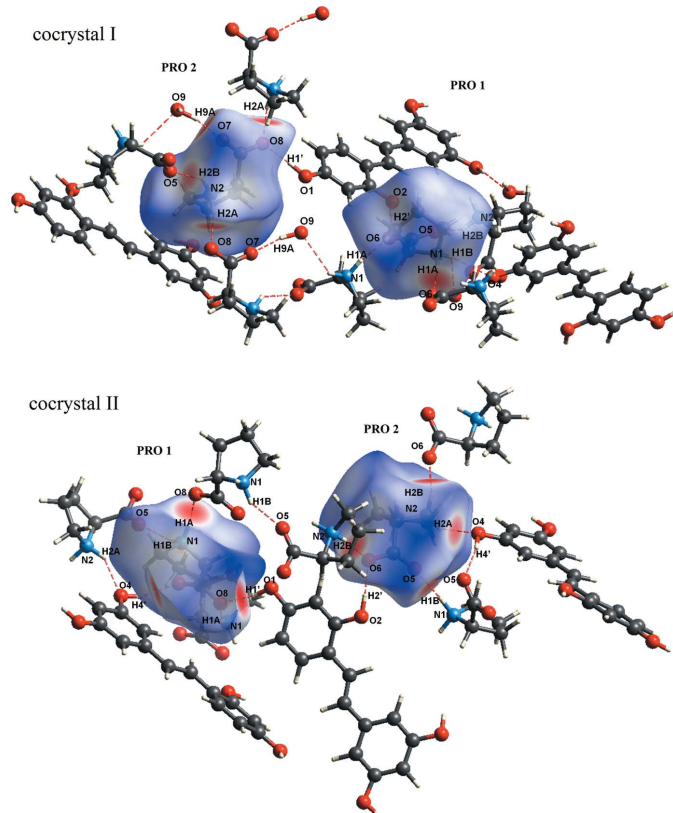


Figure 4
Hirshfeld surfaces of the PRO molecules in (I) and (II).

In addition, the two-dimensional fingerprint plots of the PRO molecules for (I) and (II) are illustrated in Figs. 5 and 6, showing the relative contributions of the various types of contacts to the Hirshfeld surface. The overall fingerprint plot for PRO 1 is shown in Fig. 5a and 6a and those delineated into the contacts of H···H, O···H/H···O and C···H/H···C interactions are displayed in Fig. 5b–d and 6b–d. Similarly, the overall fingerprint plot of PRO 2 of both cocrystals is presented in Fig. 5e and 6e and those delineated into individual contacts are shown in Fig. 5f–h and 6f–h. For cocrystals (I) and (II), the most significant interactions in terms to their relative percentage contributions are by H···H contacts with the second largest percentage attributed to H···O/O···H interactions in one PRO molecule and *vice versa* for the other PRO molecule. A pair of blue-colored spikes pointing towards the bottom left of the H···O/O···H contacts in Figs. 5 and 6 correlate with the important O—H···O and N—H···O

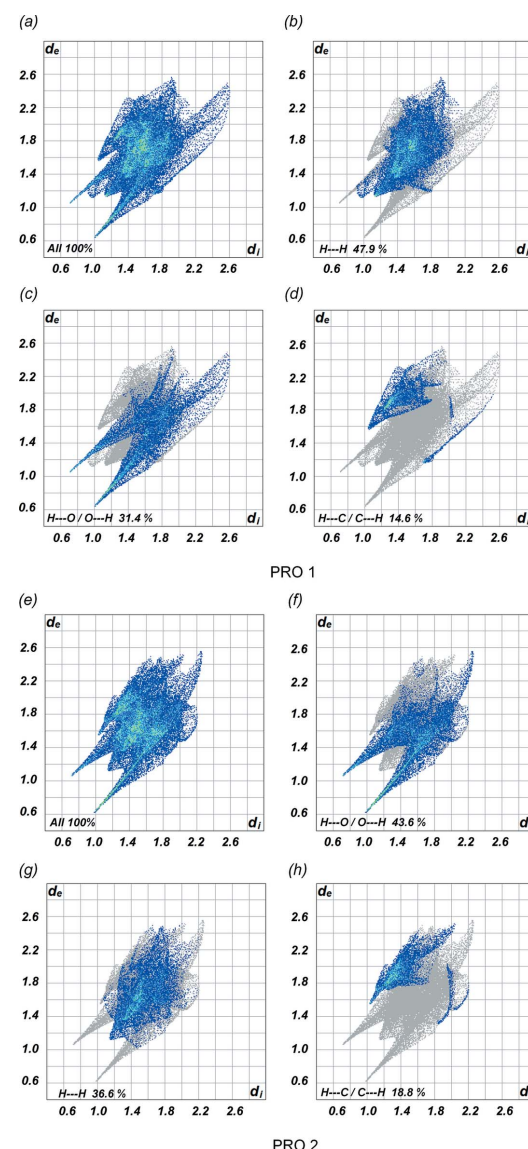


Figure 5
Fingerprint plots for the PRO molecules in (I): (a)–(d) of PRO 1 and (e)–(h) of PRO 2.

hydrogen bonds associated with the deep-red spots shown in Fig. 4. The asymmetric pair of wings for $H \cdots C/C \cdots H$ interactions in both cocrystals are also found, while other types of contact make a negligible contribution. The relative percentage contributions for the PRO 1 and PRO 2 molecules in both cocrystals are summarized in Table 3.

The OXY Hirshfeld surface, including fingerprint plots for each cocrystal, is depicted in Fig. 7. The bright-red spots on the surfaces relate to the significant hydrogen bonds of the phenolic hydroxyl groups as O donors ($O-H \cdots O$) and acceptors ($N-H \cdots O$). In (I), the hydrogen-bond contacts are observed from the O atom of the water molecule linking with the OXY surface through one of the hydroxyl groups. In addition, it is found that this water molecule is connected with PRO molecule *via* a hydrogen-bonding interaction, as indicated in part of the PRO surfaces. The fingerprint plots for OXY are illustrated below the Hirshfeld surfaces in Fig. 7a–c

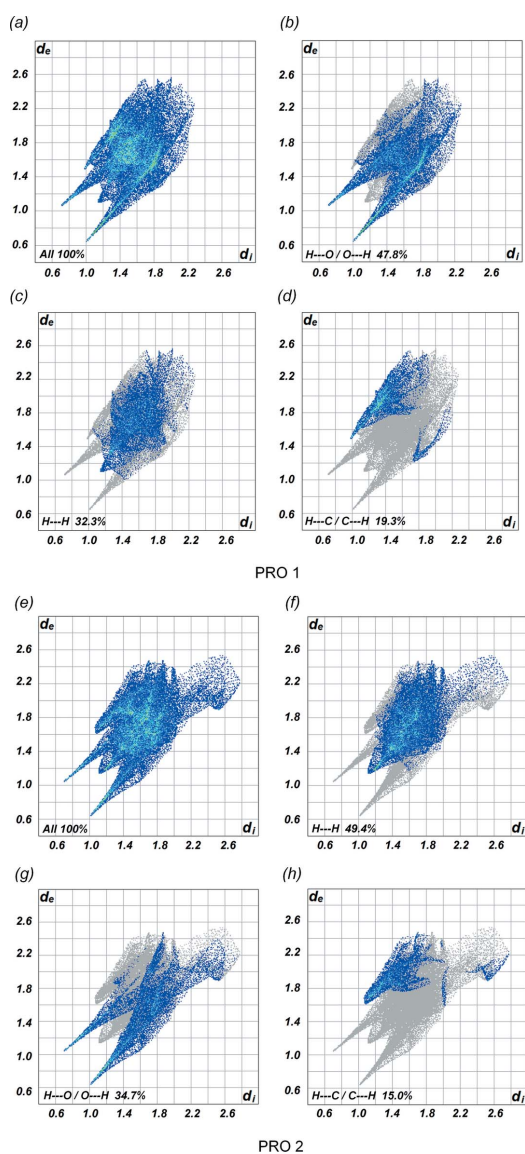


Figure 6
Fingerprint plots for the PRO molecules in (II): (a)–(d) of PRO 1 and (e)–(h) of PRO 2.

Table 3

Relative percentage contributions of close contacts of PRO and OXY molecules to the Hirshfeld surface of cocrystals I and II.

Contacts	PRO 1	PRO 2	OXY
(I)			
$H \cdots H$	47.9	36.6	38.6
$H \cdots O/O \cdots H$	31.4	43.6	33.3
$H \cdots C/C \cdots H$	14.6	18.8	–
(II)			
$H \cdots H$	32.3	49.4	38.2
$H \cdots O/O \cdots H$	47.8	34.7	35.1
$H \cdots C/C \cdots H$	19.3	15.0	–

for (I) and Fig. 7d–f for (II). The fingerprint plots Fig. 7a and Fig. 7d show the overall interactions (100%) of the OXY surface. The most significant interactions are $H \cdots H$ contacts [38.6% for (I) and 38.2% for (II)] and the second largest percentage [33.3% for (I) and 35.1% for (II)] can be attributed to $H \cdots O/O \cdots H$ contacts, which are seen as red spots on the Hirshfeld surfaces and correlate with the $O-H \cdots O$ and $N-H \cdots O$ hydrogen bonds. The relative percentage contributions of OXY are also included in Table 3. Overall, there are few differences between the Hirshfeld surfaces, fingerprint patterns and the relative percentage contributions for (I) and (II).

5. Database survey

Based on the SciFinder (2020) database, there are no reports for cocrystal structures containing OXY. Only the crystal

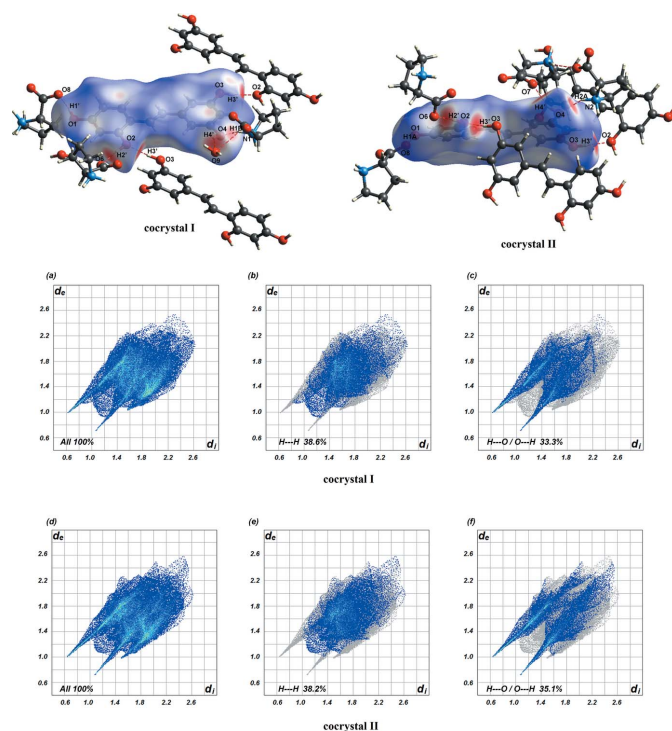


Figure 7
Hirshfeld surfaces and fingerprint plots for the OXY molecules; (a)–(c) refer to (I) and (d)–(f) refer to (II).

Table 4
Experimental details.

	(I)	(II)
Crystal data		
Chemical formula	$C_{14}H_{12}O_4 \cdot 2C_5H_9NO_2 \cdot H_2O$	$C_{14}H_{12}O_4 \cdot 2C_5H_9NO_2$
M_r	492.51	474.50
Crystal system, space group	Orthorhombic, $P2_12_12_1$	Orthorhombic, $P2_12_12_1$
Temperature (K)	297	297
a, b, c (Å)	9.9759 (2), 10.6052 (2), 22.8535 (4)	9.8293 (2), 10.4915 (2), 22.9863 (6)
V (Å ³)	2417.82 (8)	2370.44 (9)
Z	4	4
Radiation type	Mo $K\alpha$	Mo $K\alpha$
μ (mm ⁻¹)	0.10	0.10
Crystal size (mm)	0.33 × 0.23 × 0.11	0.46 × 0.33 × 0.19
Data collection		
Diffractometer	Bruker D8 VENTURE	Bruker D8 VENTURE
Absorption correction	Multi-scan (<i>SADABS</i> ; Bruker, 2016)	Multi-scan (<i>SADABS</i> ; Bruker, 2016)
T_{min}, T_{max}	0.716, 0.746	0.656, 0.747
No. of measured, independent and observed [$I > 2\sigma(I)$] reflections	27568, 4237, 4046	22887, 4084, 4038
R_{int}	0.024	0.019
(sin θ/λ) _{max} (Å ⁻¹)	0.595	0.594
Refinement		
$R[F^2 > 2\sigma(F^2)], wR(F^2), S$	0.044, 0.117, 1.05	0.047, 0.134, 1.09
No. of reflections	4237	4084
No. of parameters	332	317
No. of restraints	4	2
H-atom treatment	H atoms treated by a mixture of independent and constrained refinement	H atoms treated by a mixture of independent and constrained refinement
$\Delta\rho_{\text{max}}, \Delta\rho_{\text{min}}$ (e Å ⁻³)	0.35, -0.31	0.62, -0.22

Computer programs: *APEX2* and *SAINT* (Bruker, 2016), *SHELXT2014* (Sheldrick, 2015a), *SHELXL2018/3* (Sheldrick, 2015b), *Mercury* (Macrae *et al.*, 2020), *WinGX* (Farrugia, 2012) and *publCIF* (Westrip, 2010).

structure of OXY dihydrate was previously reported (Deng *et al.*, 2012; Cambridge Structural Database refcode ZAPDOL). The connecting C=C bond of OXY has a *trans* configuration and allows the setup of a conjugated system throughout the OXY molecule. Furthermore, in the crystal, the OXY molecules are connected through O—H···O hydrogen bonds between the hydroxy groups of OXY and water molecules. The anhydrous and monohydrate crystals of PRO have been reported in numerous papers (Seijas *et al.*, 2010; Janczak & Luger, 1997; Verbist *et al.*, 1972; Caetano *et al.*, 2018; Koenig *et al.*, 2018) and PRO invariably crystallizes in the zwitterionic form.

A search for cocrystal structures of PRO gave 148 hits. PRO has been used as a cocrystal former of various active pharmaceutical ingredients (Tilborg *et al.*, 2013; Tumanova *et al.*, 2018; Song *et al.*, 2019). The most relevant cocrystal structure to this work is the cocrystal of RES and PRO (He *et al.*, 2017; refcode PEBZEE). RES and PRO form O—H···O hydrogen bonds in the cocrystal.

6. Synthesis and crystallization

OXY and PRO were purchased from Chengdu Biopurify Phytochemicals Ltd. (Sichuan, China) and Sigma Aldrich (St. Louis, MO, USA), respectively. All organic solvents used were of analytical grade and were purchased from RCI Labscan Ltd (Bangkok, Thailand). All chemicals and solvents were used as

received without further purification. Solid OXY (122.10 mg, 0.50 mmol) and PRO (115.10 mg, 1.00 mmol) were added to a 20 ml transparent glass vial. To this was added a mixture of methanol and acetonitrile (1:1 *v/v*, 12 ml), followed by sonication until all solids were entirely dissolved. The mixture was divided into two portions, and each was covered with aluminum foil with a few small holes in it. Crystals of (I) in the form of colourless rods were obtained when the solution was placed on a hot plate at 323 K for 16 h. Single crystals of (II) (colourless blocks) were grown from a solution that was left at room temperature (303 K) for 16 h.

7. Refinement

Crystal data, data collection and structure refinement details for (I) and (II) are summarized in Table 4. The H atoms of PRO molecules of both cocrystals were included with calculated positions and isotropically refined with $U_{\text{iso}}(\text{H}) = 1.2U_{\text{eq}}(\text{N})$. However, two H atoms on phenolic hydroxyl groups for OXY [for (I) and (II)] and water [for (I)] were located in difference maps and isotropically refined with the distance restraint O—H = 0.82 (2)–0.89 (2) Å for OXY and O—H = 0.89 (2)–1.03 (2) Å for water. The other two H atoms of the OXY molecules were calculated and isotropically refined and the constraint with $U_{\text{iso}}(\text{H}) = 1.5U_{\text{eq}}(\text{O})$ was applied.

Funding information

The authors thank the Thailand Research Fund for financial support through the Royal Golden Jubilee PhD Program (grant No. PHD/0160/2558) and the Integrated Research and Development of Medicine Project (grant No. PHA610372S).

References

- Bruker (2016). *APEX2, SAINT and SADABS*. Bruker AXS Inc., Madison, Wisconsin, USA.
- Caetano *et al.* (2018). Please supply missing reference.
- Chao, J., Yu, M.-S., Ho, Y.-S., Wang, M. & Chang, R. C.-C. (2008). *Free Radical Biol. Med.* **45**, 1019–1026.
- Chesna, A. M., Cox, J. M., Basso, S. & Benedict, J. B. (2017). *Acta Cryst. E73*, 369–371.
- Deng, H., He, X., Xu, Y. & Hu, X. (2012). *Acta Cryst. E68*, o1318–o1319.
- Farrugia, L. J. (2012). *J. Appl. Cryst.* **45**, 849–854.
- He, H., Huang, Y., Zhang, Q., Wang, J.-R. & Mei, X. (2016). *Cryst. Growth Des.* **16**, 2348–2356.
- He, H. Y., Zhang, Q., Li, M. Q., Wang, J. R. & Mei, X. F. (2017). *Cryst. Growth Des.* **17**, 3989–3996.
- Janczak, J. & Luger, P. (1997). *Acta Cryst. C53*, 1954–1956.
- Jia, Y.-N., Lu, H.-P., Peng, Y.-L., Zhang, B.-S., Gong, X.-B., Su, J., Zhou, Y., Pan, M.-H. & Xu, L. (2018). *Int. Immunopharmacol.* **56**, 105–112.
- Koenig, J. J., Neudörfl, J.-M., Hansen, A. & Breugst, M. (2018). *Acta Cryst. E74*, 1067–1070.
- Lu, H.-P., Jia, Y.-N., Peng, Y.-L., Yu, Y., Sun, S.-L., Yue, M.-T., Pan, M.-H., Zeng, L.-S. & Xu, L. (2017). *Phytother. Res.* **31**, 1842–1848.
- Macrae, C. F., Sovago, I., Cottrell, S. J., Galek, P. T. A., McCabe, P., Pidcock, E., Platings, M., Shields, G. P., Stevens, J. S., Towler, M. & Wood, P. A. (2020). *J. Appl. Cryst.* **53**, 226–235.
- McKinnon, J. J., Jayatilaka, D. & Spackman, M. A. (2007). *Chem. Commun.* pp. 3814–3816.
- McKinnon, J. J., Spackman, M. A. & Mitchell, A. S. (2004). *Acta Cryst. B60*, 627–668.
- Panday, S. K. (2011). *Tetrahedron Asymmetry*, **22**, 1817–1847.
- SciFinder (2020). Chemical Abstracts Service: Columbus, OH, 2010; RN 58-08-2 (accessed March 2020).
- Sejas, L. E., Delgado, G. E., Mora, A. J., Fitch, A. N. & Brunelli, M. (2010). *Powder Diffr.* **25**, 235–240.
- Shah, A., Chao, J., Legido-Quigley, C. & Chang, R. C.-C. (2019). *Nutr. Neurosci.* pp. 1–16.
- Sheldrick, G. M. (2015a). *Acta Cryst. A71*, 3–8.
- Sheldrick, G. M. (2015b). *Acta Cryst. C71*, 3–8.
- Song, Y., Wang, L.-Y., Liu, F., Li, Y.-T., Wu, Z.-Y. & Yan, C.-W. (2019). *CrystEngComm*, **21**, 3064–3073.
- Spackman, M. A. & Jayatilaka, D. (2009). *CrystEngComm*, **11**, 19–32.
- Surov, A. O., Voronin, A. P., Vener, M. V., Churakov, A. V. & Perlovich, G. L. (2018). *CrystEngComm*, **20**, 6970–6981.
- Suzuki, Y., Muangnoi, C., Thaweesest, W., Teerawonganapan, P., Ratnatilaka Na Bhuket, P., Titapiwatanakun, V., Yoshimura-Fujii, M., Sritularak, B., Likhitwitayawuid, K., Rojsitthisak, P. & Fukami, T. (2019). *Biol. Pharm. Bull.* **42**, 1004–1012.
- Tilborg, A., Norberg, B. & Wouters, J. (2014). *Eur. J. Med. Chem.* **74**, 411–426.
- Tilborg, A., Springuel, G., Norberg, B., Wouters, J. & Leyssens, T. (2013). *CrystEngComm*, **15**, 3341–3350.
- Tumanova, N., Tumanov, N., Fischer, F., Morelle, F., Ban, V., Robeyns, K., Filinchuk, Y., Wouters, J., Emmerling, F. & Leyssens, T. (2018). *CrystEngComm*, **20**, 7308–7321.
- Turner, M. J., Mckinnon, J. J., Wolff, S. K., Grimwood, D. J., Spackman, P. R., Jayatilaka, D. & Spackman, M. A. (2017). *CrystaExplor17.5*. The University of Western Australia.
- Verbist, J. J., Lehmann, M. S., Koetzle, T. F. & Hamilton, W. C. (1972). *Nature*, **235**, 328–329.
- Westrip, S. P. (2010). *J. Appl. Cryst.* **43**, 920–925.

supporting information

Acta Cryst. (2020). E76, 1528-1534 [https://doi.org/10.1107/S2056989020011536]

Syntheses and crystal structures of hydrated and anhydrous 1:2 cocrystals of oxyresveratrol and zwitterionic proline

Passaporn Ouiyangkul, Saowanit Saithong and Vimol Tantishaiyakul

Computing details

For both structures, data collection: *APEX2* (Bruker, 2016); cell refinement: *SAINT* (Bruker, 2016); data reduction: *SAINT* (Bruker, 2016); program(s) used to solve structure: *SHELXT2014* (Sheldrick, 2015a); program(s) used to refine structure: *SHELXL2018/3* (Sheldrick, 2015b); molecular graphics: *Mercury* (Macrae *et al.*, 2020); software used to prepare material for publication: *WinGX* (Farrugia, 2012) and *publCIF* (Westrip, 2010).

4-[*(E*)-2-(3,5-Dihydroxyphenyl)ethenyl]benzene-1,3-diol bis[(*S*)-pyrrolidin-1-ium-2-carboxylate] monohydrate (I)

Crystal data



$M_r = 492.51$

Orthorhombic, $P2_12_12_1$

$a = 9.9759 (2) \text{ \AA}$

$b = 10.6052 (2) \text{ \AA}$

$c = 22.8535 (4) \text{ \AA}$

$V = 2417.82 (8) \text{ \AA}^3$

$Z = 4$

$F(000) = 1048$

$D_x = 1.353 \text{ Mg m}^{-3}$

Mo $K\alpha$ radiation, $\lambda = 0.71073 \text{ \AA}$

Cell parameters from 9870 reflections

$\theta = 3.3\text{--}27.2^\circ$

$\mu = 0.10 \text{ mm}^{-1}$

$T = 297 \text{ K}$

Rod, colourless

$0.33 \times 0.23 \times 0.11 \text{ mm}$

Data collection

Bruker D8 VENTURE
diffractometer

Radiation source: Sealed x-ray tube

GraphiteDouble Bounce Multilayer Mirror
monochromator

Detector resolution: 7.39 pixels mm^{-1}

φ and ω scans

Absorption correction: multi-scan
(SADABS; Bruker, 2016)

$T_{\min} = 0.716, T_{\max} = 0.746$

27568 measured reflections

4237 independent reflections

4046 reflections with $I > 2\sigma(I)$

$R_{\text{int}} = 0.024$

$\theta_{\max} = 25.0^\circ, \theta_{\min} = 2.9^\circ$

$h = -11 \rightarrow 11$

$k = -12 \rightarrow 12$

$l = -27 \rightarrow 27$

Refinement

Refinement on F^2

Least-squares matrix: full

$R[F^2 > 2\sigma(F^2)] = 0.044$

$wR(F^2) = 0.117$

$S = 1.05$

4237 reflections

332 parameters

4 restraints

Primary atom site location: structure-invariant
direct methods

Secondary atom site location: difference Fourier
map

Hydrogen site location: mixed

H atoms treated by a mixture of independent
and constrained refinement

$w = 1/[\sigma^2(F_o^2) + (0.0603P)^2 + 1.0192P]$
where $P = (F_o^2 + 2F_c^2)/3$

$(\Delta/\sigma)_{\max} < 0.001$

$\Delta\rho_{\max} = 0.35 \text{ e \AA}^{-3}$

$\Delta\rho_{\min} = -0.31 \text{ e \AA}^{-3}$

Special details

Geometry. All esds (except the esd in the dihedral angle between two l.s. planes) are estimated using the full covariance matrix. The cell esds are taken into account individually in the estimation of esds in distances, angles and torsion angles; correlations between esds in cell parameters are only used when they are defined by crystal symmetry. An approximate (isotropic) treatment of cell esds is used for estimating esds involving l.s. planes.

Fractional atomic coordinates and isotropic or equivalent isotropic displacement parameters (\AA^2)

	<i>x</i>	<i>y</i>	<i>z</i>	$U_{\text{iso}}^*/U_{\text{eq}}$
O1	0.1315 (3)	0.6159 (2)	0.61582 (10)	0.0526 (7)
N1	0.7751 (3)	0.3182 (3)	0.47097 (13)	0.0448 (7)
H1A	0.821241	0.251273	0.483057	0.054*
H1B	0.765150	0.313168	0.432344	0.054*
C1	0.1165 (3)	0.6442 (3)	0.55821 (13)	0.0380 (7)
O2	0.2661 (2)	0.5415 (2)	0.42047 (10)	0.0456 (6)
H2'	0.323 (4)	0.489 (4)	0.4405 (11)	0.068*
N2	-0.0782 (3)	0.4926 (2)	0.79401 (11)	0.0366 (6)
H2A	-0.032399	0.421409	0.799100	0.044*
H2B	-0.055795	0.546139	0.822364	0.044*
C2	0.0261 (4)	0.7335 (3)	0.53867 (14)	0.0459 (8)
H2	-0.026401	0.778272	0.565113	0.055*
O3	-0.2666 (3)	0.9933 (3)	0.19900 (11)	0.0567 (7)
C3	0.0150 (4)	0.7553 (3)	0.47947 (14)	0.0484 (8)
H3	-0.047640	0.814001	0.466565	0.058*
O4	0.0969 (5)	0.7386 (4)	0.13945 (13)	0.0928 (13)
H4'	0.190 (8)	0.723 (8)	0.1526 (16)	0.139*
C4	0.0942 (3)	0.6928 (3)	0.43769 (13)	0.0369 (7)
O5	0.5778 (3)	0.4212 (3)	0.41114 (10)	0.0520 (6)
C5	0.1858 (3)	0.6041 (3)	0.45910 (12)	0.0323 (6)
O6	0.4180 (2)	0.3743 (2)	0.47524 (11)	0.0489 (6)
C6	0.1957 (3)	0.5792 (3)	0.51887 (13)	0.0354 (6)
H6	0.255747	0.518732	0.532283	0.042*
O7	-0.0442 (5)	0.7425 (2)	0.78719 (12)	0.0891 (13)
C7	0.0819 (4)	0.7181 (3)	0.37485 (14)	0.0426 (7)
H7	0.147494	0.684006	0.350660	0.051*
O8	-0.0014 (3)	0.7457 (2)	0.69276 (10)	0.0562 (7)
C8	-0.0133 (4)	0.7847 (4)	0.34932 (14)	0.0450 (8)
H8	-0.078062	0.818540	0.374046	0.054*
O9	0.3312 (5)	0.6407 (4)	0.1266 (2)	0.0987 (14)
C9	-0.0299 (3)	0.8120 (3)	0.28670 (14)	0.0391 (7)
C10	-0.1353 (3)	0.8902 (3)	0.27012 (14)	0.0418 (7)
H10	-0.190263	0.925334	0.298660	0.050*
C11	-0.1595 (3)	0.9162 (3)	0.21180 (14)	0.0426 (7)
C12	-0.0792 (4)	0.8656 (4)	0.16910 (15)	0.0519 (9)
H12	-0.094718	0.884207	0.129914	0.062*
C13	0.0242 (4)	0.7874 (4)	0.18468 (15)	0.0548 (9)
C14	0.0517 (4)	0.7593 (3)	0.24318 (15)	0.0472 (8)
H14	0.122696	0.706643	0.253042	0.057*

C15	0.5376 (3)	0.3770 (3)	0.45739 (13)	0.0357 (7)
C16	0.6412 (3)	0.3223 (3)	0.50027 (14)	0.0378 (7)
H16	0.614353	0.237957	0.513251	0.045*
C17	0.6655 (4)	0.4086 (5)	0.55262 (16)	0.0623 (11)
H17A	0.583267	0.450158	0.564463	0.075*
H17B	0.700761	0.361392	0.585567	0.075*
C18	0.7653 (6)	0.5017 (6)	0.5311 (3)	0.0917 (17)
H18A	0.720375	0.573782	0.513840	0.110*
H18B	0.821256	0.530953	0.563023	0.110*
C19	0.8472 (5)	0.4362 (5)	0.4868 (3)	0.0820 (15)
H19A	0.935075	0.416595	0.502539	0.098*
H19B	0.858597	0.489086	0.452511	0.098*
C20	-0.0468 (3)	0.5485 (3)	0.73547 (12)	0.0331 (6)
H20	0.035826	0.510986	0.720132	0.040*
C21	-0.1645 (5)	0.5115 (4)	0.69655 (18)	0.0650 (11)
H21A	-0.210407	0.586187	0.682371	0.078*
H21B	-0.133480	0.463214	0.663169	0.078*
C22	-0.2580 (5)	0.4327 (5)	0.7340 (2)	0.0784 (14)
H22A	-0.350908	0.452288	0.725335	0.094*
H22B	-0.243179	0.343458	0.727209	0.094*
C23	-0.2245 (4)	0.4669 (4)	0.7956 (2)	0.0656 (11)
H23A	-0.273919	0.541110	0.807923	0.079*
H23B	-0.244741	0.397964	0.822045	0.079*
C24	-0.0301 (4)	0.6913 (3)	0.73993 (14)	0.0455 (8)
H1'	0.080 (4)	0.660 (4)	0.6361 (18)	0.068*
H3'	-0.270 (5)	1.004 (5)	0.1623 (11)	0.068*
H9A	0.376 (4)	0.670 (4)	0.1576 (14)	0.055*
H9B	0.419 (3)	0.644 (4)	0.1031 (16)	0.055*

Atomic displacement parameters (\AA^2)

	U^{11}	U^{22}	U^{33}	U^{12}	U^{13}	U^{23}
O1	0.0727 (17)	0.0544 (15)	0.0305 (11)	0.0138 (13)	0.0030 (11)	0.0011 (11)
N1	0.0333 (14)	0.0529 (17)	0.0481 (16)	0.0065 (12)	0.0018 (12)	0.0036 (13)
C1	0.0474 (18)	0.0358 (16)	0.0309 (15)	-0.0028 (14)	-0.0001 (13)	-0.0031 (12)
O2	0.0475 (13)	0.0572 (14)	0.0322 (12)	0.0176 (11)	-0.0042 (10)	-0.0039 (10)
N2	0.0513 (16)	0.0274 (12)	0.0311 (13)	-0.0006 (11)	0.0041 (11)	-0.0008 (10)
C2	0.0532 (19)	0.0458 (18)	0.0388 (17)	0.0128 (16)	0.0072 (15)	-0.0022 (14)
O3	0.0526 (15)	0.0767 (18)	0.0408 (14)	0.0061 (14)	-0.0015 (11)	0.0187 (14)
C3	0.054 (2)	0.0473 (19)	0.0439 (18)	0.0172 (16)	0.0014 (16)	0.0053 (15)
O4	0.126 (3)	0.097 (3)	0.0546 (17)	0.039 (2)	0.0386 (19)	0.0031 (18)
C4	0.0368 (16)	0.0379 (16)	0.0359 (16)	0.0031 (13)	-0.0006 (13)	-0.0006 (13)
O5	0.0557 (14)	0.0676 (16)	0.0326 (11)	0.0066 (12)	0.0033 (11)	0.0128 (11)
C5	0.0310 (14)	0.0343 (15)	0.0316 (14)	-0.0030 (12)	-0.0022 (11)	-0.0052 (12)
O6	0.0313 (12)	0.0589 (15)	0.0565 (14)	0.0063 (11)	0.0013 (10)	0.0141 (12)
C6	0.0351 (15)	0.0371 (15)	0.0339 (15)	0.0014 (12)	-0.0054 (12)	0.0003 (13)
O7	0.191 (4)	0.0338 (13)	0.0430 (14)	-0.0075 (19)	0.031 (2)	-0.0107 (12)
C7	0.0484 (18)	0.0435 (18)	0.0358 (16)	0.0078 (15)	0.0034 (14)	0.0017 (14)

O8	0.099 (2)	0.0303 (11)	0.0394 (12)	-0.0038 (13)	0.0118 (13)	0.0020 (10)
C8	0.0436 (18)	0.056 (2)	0.0360 (17)	0.0085 (16)	0.0019 (14)	0.0033 (15)
O9	0.109 (3)	0.072 (2)	0.115 (3)	0.016 (2)	-0.056 (3)	-0.022 (2)
C9	0.0418 (16)	0.0414 (17)	0.0341 (15)	-0.0007 (14)	0.0015 (14)	0.0045 (13)
C10	0.0434 (17)	0.0479 (18)	0.0341 (16)	0.0007 (15)	0.0058 (13)	0.0057 (14)
C11	0.0456 (18)	0.0458 (18)	0.0363 (16)	-0.0069 (15)	-0.0001 (14)	0.0074 (14)
C12	0.072 (2)	0.052 (2)	0.0313 (16)	-0.0028 (19)	0.0020 (16)	0.0065 (15)
C13	0.074 (2)	0.0491 (19)	0.0411 (19)	0.0025 (19)	0.0206 (18)	0.0002 (16)
C14	0.054 (2)	0.0429 (18)	0.0449 (18)	0.0043 (15)	0.0050 (16)	0.0058 (15)
C15	0.0348 (16)	0.0383 (16)	0.0340 (16)	0.0034 (13)	-0.0010 (12)	0.0005 (13)
C16	0.0318 (15)	0.0457 (18)	0.0357 (15)	0.0007 (13)	0.0013 (13)	0.0089 (13)
C17	0.057 (2)	0.095 (3)	0.0356 (18)	0.000 (2)	-0.0052 (16)	-0.005 (2)
C18	0.092 (4)	0.094 (4)	0.088 (4)	-0.028 (3)	0.004 (3)	-0.033 (3)
C19	0.053 (2)	0.058 (3)	0.135 (5)	-0.012 (2)	0.018 (3)	0.000 (3)
C20	0.0461 (17)	0.0274 (13)	0.0259 (13)	0.0006 (12)	0.0021 (12)	-0.0016 (11)
C21	0.079 (3)	0.065 (3)	0.051 (2)	-0.018 (2)	-0.023 (2)	0.003 (2)
C22	0.062 (3)	0.077 (3)	0.096 (4)	-0.022 (2)	-0.018 (2)	0.004 (3)
C23	0.053 (2)	0.069 (3)	0.075 (3)	-0.005 (2)	0.015 (2)	0.007 (2)
C24	0.073 (2)	0.0290 (15)	0.0341 (16)	0.0016 (15)	0.0058 (16)	-0.0039 (13)

Geometric parameters (\AA , $^{\circ}$)

O1—C1	1.359 (4)	O9—H9A	0.89 (2)
O1—H1'	0.84 (2)	O9—H9B	1.03 (2)
N1—C19	1.487 (6)	C9—C10	1.392 (5)
N1—C16	1.495 (4)	C9—C14	1.401 (5)
N1—H1A	0.8900	C10—C11	1.382 (4)
N1—H1B	0.8900	C10—H10	0.9300
C1—C6	1.381 (5)	C11—C12	1.372 (5)
C1—C2	1.382 (5)	C12—C13	1.370 (6)
O2—C5	1.364 (4)	C12—H12	0.9300
O2—H2'	0.92 (5)	C13—C14	1.397 (5)
N2—C23	1.486 (5)	C13—H14	0.9300
N2—C20	1.496 (4)	C14—C16	1.538 (4)
N2—H2A	0.8900	C15—C16	1.525 (5)
N2—H2B	0.8900	C16—C17	0.9800
C2—C3	1.377 (5)	C16—H16	1.486 (7)
C2—H2	0.9300	C17—C18	0.9700
O3—C11	1.378 (4)	C17—H17A	0.9700
O3—H3'	0.85 (2)	C17—H17B	0.9700
C3—C4	1.405 (5)	C18—C19	1.475 (8)
C3—H3	0.9300	C18—H18A	0.9700
O4—C13	1.365 (4)	C18—H18B	0.9700
O4—H4'	0.99 (8)	C19—H19A	0.9700
C4—C5	1.400 (4)	C19—H19B	0.9700
C4—C7	1.466 (4)	C20—C21	1.525 (5)
O5—C15	1.224 (4)	C20—C24	1.526 (4)
C5—C6	1.395 (4)	C20—H20	0.9800
		C21—C22	1.517 (6)

O6—C15	1.262 (4)	C21—H21A	0.9700
C6—H6	0.9300	C21—H21B	0.9700
O7—C24	1.217 (4)	C22—C23	1.492 (7)
C7—C8	1.319 (5)	C22—H22A	0.9700
C7—H7	0.9300	C22—H22B	0.9700
O8—C24	1.256 (4)	C23—H23A	0.9700
C8—C9	1.469 (4)	C23—H23B	0.9700
C8—H8	0.9300		
C1—O1—H1'	110 (3)	C13—C14—H14	120.6
C19—N1—C16	107.4 (3)	C9—C14—H14	120.6
C19—N1—H1A	110.2	O5—C15—O6	126.7 (3)
C16—N1—H1A	110.2	O5—C15—C16	118.3 (3)
C19—N1—H1B	110.2	O6—C15—C16	114.9 (3)
C16—N1—H1B	110.2	N1—C16—C17	103.1 (3)
H1A—N1—H1B	108.5	N1—C16—C15	109.0 (2)
O1—C1—C6	117.2 (3)	C17—C16—C15	112.4 (3)
O1—C1—C2	122.5 (3)	N1—C16—H16	110.7
C6—C1—C2	120.3 (3)	C17—C16—H16	110.7
C5—O2—H2'	109.5	C15—C16—H16	110.7
C23—N2—C20	107.5 (3)	C18—C17—C16	104.2 (3)
C23—N2—H2A	110.2	C18—C17—H17A	110.9
C20—N2—H2A	110.2	C16—C17—H17A	110.9
C23—N2—H2B	110.2	C18—C17—H17B	110.9
C20—N2—H2B	110.2	C16—C17—H17B	110.9
H2A—N2—H2B	108.5	H17A—C17—H17B	108.9
C3—C2—C1	119.0 (3)	C19—C18—C17	106.6 (4)
C3—C2—H2	120.5	C19—C18—H18A	110.4
C1—C2—H2	120.5	C17—C18—H18A	110.4
C11—O3—H3'	109 (3)	C19—C18—H18B	110.4
C2—C3—C4	122.9 (3)	C17—C18—H18B	110.4
C2—C3—H3	118.6	H18A—C18—H18B	108.6
C4—C3—H3	118.6	C18—C19—N1	107.2 (4)
C13—O4—H4'	109.5	C18—C19—H19A	110.3
C5—C4—C3	116.5 (3)	N1—C19—H19A	110.3
C5—C4—C7	121.3 (3)	C18—C19—H19B	110.3
C3—C4—C7	122.2 (3)	N1—C19—H19B	110.3
O2—C5—C6	120.0 (3)	H19A—C19—H19B	108.5
O2—C5—C4	119.0 (3)	N2—C20—C21	105.0 (3)
C6—C5—C4	121.0 (3)	N2—C20—C24	110.9 (2)
C1—C6—C5	120.2 (3)	C21—C20—C24	112.2 (3)
C1—C6—H6	119.9	N2—C20—H20	109.6
C5—C6—H6	119.9	C21—C20—H20	109.6
C8—C7—C4	126.2 (3)	C24—C20—H20	109.6
C8—C7—H7	116.9	C22—C21—C20	106.6 (3)
C4—C7—H7	116.9	C22—C21—H21A	110.4
C7—C8—C9	128.1 (3)	C20—C21—H21A	110.4
C7—C8—H8	116.0	C22—C21—H21B	110.4

C9—C8—H8	116.0	C20—C21—H21B	110.4
H9A—O9—H9B	89 (3)	H21A—C21—H21B	108.6
C10—C9—C14	118.9 (3)	C23—C22—C21	105.1 (3)
C10—C9—C8	117.9 (3)	C23—C22—H22A	110.7
C14—C9—C8	123.2 (3)	C21—C22—H22A	110.7
C11—C10—C9	120.9 (3)	C23—C22—H22B	110.7
C11—C10—H10	119.6	C21—C22—H22B	110.7
C9—C10—H10	119.6	H22A—C22—H22B	108.8
C12—C11—O3	122.3 (3)	N2—C23—C22	104.0 (3)
C12—C11—C10	120.4 (3)	N2—C23—H23A	111.0
O3—C11—C10	117.3 (3)	C22—C23—H23A	111.0
C13—C12—C11	119.4 (3)	N2—C23—H23B	111.0
C13—C12—H12	120.3	C22—C23—H23B	111.0
C11—C12—H12	120.3	H23A—C23—H23B	109.0
O4—C13—C12	115.6 (3)	O7—C24—O8	125.7 (3)
O4—C13—C14	122.7 (4)	O7—C24—C20	119.3 (3)
C12—C13—C14	121.7 (3)	O8—C24—C20	115.0 (3)
C13—C14—C9	118.7 (3)		
O1—C1—C2—C3	-178.9 (3)	O4—C13—C14—C9	-178.9 (4)
C6—C1—C2—C3	0.9 (5)	C12—C13—C14—C9	0.6 (6)
C1—C2—C3—C4	-1.6 (6)	C10—C9—C14—C13	0.1 (5)
C2—C3—C4—C5	0.8 (5)	C8—C9—C14—C13	177.5 (4)
C2—C3—C4—C7	-179.4 (4)	C19—N1—C16—C17	-25.4 (4)
C3—C4—C5—O2	-179.4 (3)	C19—N1—C16—C15	94.1 (4)
C7—C4—C5—O2	0.8 (5)	O5—C15—C16—N1	-8.3 (4)
C3—C4—C5—C6	0.7 (5)	O6—C15—C16—N1	173.7 (3)
C7—C4—C5—C6	-179.1 (3)	O5—C15—C16—C17	105.3 (4)
O1—C1—C6—C5	-179.7 (3)	O6—C15—C16—C17	-72.7 (4)
C2—C1—C6—C5	0.5 (5)	N1—C16—C17—C18	33.9 (4)
O2—C5—C6—C1	178.7 (3)	C15—C16—C17—C18	-83.3 (4)
C4—C5—C6—C1	-1.4 (5)	C16—C17—C18—C19	-30.2 (6)
C5—C4—C7—C8	169.2 (4)	C17—C18—C19—N1	14.5 (6)
C3—C4—C7—C8	-10.6 (6)	C16—N1—C19—C18	7.3 (6)
C4—C7—C8—C9	-179.7 (3)	C23—N2—C20—C21	-19.7 (4)
C7—C8—C9—C10	-176.9 (4)	C23—N2—C20—C24	101.7 (3)
C7—C8—C9—C14	5.8 (6)	N2—C20—C21—C22	-1.4 (4)
C14—C9—C10—C11	-0.3 (5)	C24—C20—C21—C22	-121.9 (4)
C8—C9—C10—C11	-177.7 (3)	C20—C21—C22—C23	21.6 (5)
C9—C10—C11—C12	-0.3 (5)	C20—N2—C23—C22	33.4 (4)
C9—C10—C11—O3	179.3 (3)	C21—C22—C23—N2	-33.4 (5)
O3—C11—C12—C13	-178.7 (3)	N2—C20—C24—O7	-0.7 (5)
C10—C11—C12—C13	1.0 (5)	C21—C20—C24—O7	116.3 (4)
C11—C12—C13—O4	178.4 (4)	N2—C20—C24—O8	178.9 (3)
C11—C12—C13—C14	-1.1 (6)	C21—C20—C24—O8	-64.1 (5)

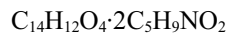
Hydrogen-bond geometry (\AA , $^\circ$)

$D\cdots H$	$D\cdots H$	$H\cdots A$	$D\cdots A$	$D\cdots H\cdots A$
O1—H1'…O8	0.84 (2)	1.78 (3)	2.597 (3)	166 (5)
O2—H2'…O6	0.92	1.74	2.647 (3)	172
O3—H3'…O2 ⁱ	0.85 (2)	1.93 (3)	2.778 (3)	175 (5)
O4—H4'…O9	0.99	1.76	2.575 (6)	137
O9—H9A…O7 ⁱⁱ	0.89 (2)	1.76 (3)	2.639 (5)	168 (4)
N1—H1A…O6 ⁱⁱⁱ	0.89	1.90	2.777 (4)	168
N1—H1B…O4 ^{iv}	0.89	2.28	2.951 (4)	132
N1—H1B…O9 ^{iv}	0.89	2.47	3.105 (5)	129
N2—H2A…O8 ^v	0.89	1.90	2.753 (3)	159
N2—H2B…O5 ^{vi}	0.89	2.07	2.829 (3)	143
N2—H2B…O7	0.89	2.24	2.677 (4)	110
C6—H6…O6	0.93	2.58	3.261 (4)	130
C12—H12…O2 ⁱ	0.93	2.65	3.339 (5)	131

Symmetry codes: (i) $-x, y+1/2, -z+1/2$; (ii) $x+1/2, -y+3/2, -z+1$; (iii) $x+1/2, -y+1/2, -z+1$; (iv) $-x+1, y-1/2, -z+1/2$; (v) $-x, y-1/2, -z+3/2$; (vi) $-x+1/2, -y+1, z+1/2$.

4-[(*E*)-2-(3,5-Dihydroxyphenyl)ethenyl]benzene-1,3-diol bis[(*S*)-pyrrolidin-1-iun-2-carboxylate] (II)

Crystal data

 $M_r = 474.50$ Orthorhombic, $P2_12_12_1$ $a = 9.8293 (2) \text{\AA}$ $b = 10.4915 (2) \text{\AA}$ $c = 22.9863 (6) \text{\AA}$ $V = 2370.44 (9) \text{\AA}^3$ $Z = 4$ $F(000) = 1008$ $D_x = 1.330 \text{ Mg m}^{-3}$ Mo $K\alpha$ radiation, $\lambda = 0.71073 \text{\AA}$

Cell parameters from 9885 reflections

 $\theta = 3.0\text{--}33.7^\circ$ $\mu = 0.10 \text{ mm}^{-1}$ $T = 297 \text{ K}$

Block, colourless

 $0.46 \times 0.33 \times 0.19 \text{ mm}$

Data collection

Bruker D8 VENTURE
diffractometer

Radiation source: Sealed x-ray tube

GraphiteDouble Bounce Multilayer Mirror
monochromatorDetector resolution: 7.39 pixels mm^{-1} φ and ω scansAbsorption correction: multi-scan
(SADABS; Bruker, 2016) $T_{\min} = 0.656, T_{\max} = 0.747$

22887 measured reflections

4084 independent reflections

4038 reflections with $I > 2\sigma(I)$ $R_{\text{int}} = 0.019$ $\theta_{\max} = 25.0^\circ, \theta_{\min} = 3.0^\circ$ $h = -11 \rightarrow 11$ $k = -12 \rightarrow 12$ $l = -27 \rightarrow 27$

Refinement

Refinement on F^2

Least-squares matrix: full

 $R[F^2 > 2\sigma(F^2)] = 0.047$ $wR(F^2) = 0.134$ $S = 1.09$

4084 reflections

317 parameters

2 restraints

Primary atom site location: structure-invariant
direct methodsSecondary atom site location: difference Fourier
map

Hydrogen site location: mixed

H atoms treated by a mixture of independent
and constrained refinement $w = 1/[\sigma^2(F_o^2) + (0.0845P)^2 + 0.7969P]$
where $P = (F_o^2 + 2F_c^2)/3$ $(\Delta/\sigma)_{\max} < 0.001$ $\Delta\rho_{\max} = 0.62 \text{ e \AA}^{-3}$ $\Delta\rho_{\min} = -0.22 \text{ e \AA}^{-3}$

Special details

Geometry. All esds (except the esd in the dihedral angle between two l.s. planes) are estimated using the full covariance matrix. The cell esds are taken into account individually in the estimation of esds in distances, angles and torsion angles; correlations between esds in cell parameters are only used when they are defined by crystal symmetry. An approximate (isotropic) treatment of cell esds is used for estimating esds involving l.s. planes.

Fractional atomic coordinates and isotropic or equivalent isotropic displacement parameters (\AA^2)

	<i>x</i>	<i>y</i>	<i>z</i>	$U_{\text{iso}}*/U_{\text{eq}}$
O1	0.1260 (3)	0.6128 (3)	0.61986 (10)	0.0514 (7)
H1'	0.071 (6)	0.669 (5)	0.6427 (14)	0.077*
N1	-0.0705 (3)	0.4844 (2)	0.79572 (11)	0.0353 (6)
H1A	-0.014333	0.419063	0.801444	0.042*
H1B	-0.056256	0.541800	0.823585	0.042*
C1	0.1126 (3)	0.6427 (3)	0.56307 (13)	0.0352 (7)
O2	0.2565 (2)	0.5318 (3)	0.42496 (9)	0.0427 (6)
N2	0.7837 (3)	0.3235 (3)	0.46631 (12)	0.0389 (6)
H2A	0.772557	0.318253	0.427954	0.047*
H2B	0.837980	0.260292	0.477681	0.047*
C2	0.0265 (4)	0.7382 (4)	0.54340 (14)	0.0453 (8)
H2	-0.024706	0.785813	0.569582	0.054*
O3	-0.2495 (3)	0.9798 (3)	0.19378 (11)	0.0495 (6)
H3'	-0.249 (3)	0.987 (5)	0.156 (3)	0.074*
C3	0.0180 (4)	0.7616 (4)	0.48443 (14)	0.0455 (8)
H3	-0.041818	0.824262	0.471595	0.055*
O4	0.1637 (3)	0.7502 (3)	0.15416 (11)	0.0599 (8)
C4	0.0949 (3)	0.6957 (3)	0.44306 (13)	0.0356 (7)
O5	0.5729 (3)	0.4173 (3)	0.41022 (10)	0.0533 (7)
C5	0.1812 (3)	0.6002 (3)	0.46420 (13)	0.0309 (6)
O6	0.4198 (2)	0.3686 (3)	0.47823 (11)	0.0466 (6)
C6	0.1903 (3)	0.5733 (3)	0.52325 (13)	0.0329 (6)
H6	0.247994	0.509154	0.536261	0.039*
O7	-0.0892 (3)	0.7406 (2)	0.78591 (10)	0.0460 (6)
C7	0.0875 (4)	0.7241 (3)	0.38077 (13)	0.0386 (7)
H7	0.156958	0.691646	0.357645	0.046*
O8	-0.0296 (3)	0.7428 (2)	0.69242 (10)	0.0506 (7)
C8	-0.0076 (3)	0.7910 (4)	0.35402 (14)	0.0398 (7)
H8	-0.075927	0.825377	0.377158	0.048*
C9	-0.0159 (3)	0.8164 (3)	0.29118 (14)	0.0360 (7)
C10	-0.1234 (3)	0.8909 (3)	0.27047 (14)	0.0371 (7)
H10	-0.185411	0.926232	0.296429	0.044*
C11	-0.1378 (3)	0.9121 (3)	0.21109 (14)	0.0366 (7)
C12	-0.0429 (4)	0.8644 (3)	0.17235 (13)	0.0411 (8)
H12	-0.051837	0.880042	0.132705	0.049*
C13	0.0660 (4)	0.7930 (3)	0.19307 (14)	0.0419 (7)
C14	0.0793 (4)	0.7665 (3)	0.25177 (14)	0.0399 (7)
H14	0.150671	0.716115	0.265004	0.048*
C15	0.5388 (3)	0.3722 (3)	0.45688 (13)	0.0329 (6)

C16	0.6496 (3)	0.3150 (3)	0.49651 (14)	0.0378 (7)
H16	0.628213	0.226093	0.505799	0.045*
C17	0.6714 (5)	0.3919 (6)	0.55258 (16)	0.0633 (12)
H17A	0.588047	0.434238	0.564351	0.076*
H17B	0.701960	0.337248	0.583990	0.076*
C18	0.7786 (8)	0.4871 (8)	0.5367 (3)	0.108 (3)
H18A	0.737801	0.570706	0.532318	0.130*
H18B	0.845990	0.491800	0.567471	0.130*
C19	0.8440 (5)	0.4497 (5)	0.4825 (2)	0.0664 (12)
H19A	0.941535	0.442251	0.487748	0.080*
H19B	0.826332	0.512272	0.452326	0.080*
C20	-0.0456 (3)	0.5426 (3)	0.73720 (12)	0.0326 (6)
H20	0.044694	0.517884	0.723075	0.039*
C21	-0.1553 (5)	0.4849 (4)	0.69788 (18)	0.0583 (10)
H21A	-0.208778	0.551754	0.679827	0.070*
H21B	-0.113911	0.433781	0.667490	0.070*
C22	-0.2429 (6)	0.4041 (6)	0.7356 (2)	0.0830 (17)
H22A	-0.338064	0.418173	0.726516	0.100*
H22B	-0.222303	0.314678	0.729493	0.100*
C23	-0.2149 (4)	0.4400 (4)	0.7970 (2)	0.0583 (10)
H23A	-0.225509	0.367342	0.822688	0.070*
H23B	-0.275284	0.507642	0.809722	0.070*
C24	-0.0559 (3)	0.6875 (3)	0.74016 (13)	0.0350 (7)
H2'	0.311 (4)	0.484 (4)	0.4408 (18)	0.052*
H4'	0.234 (3)	0.736 (5)	0.1775 (16)	0.052*

Atomic displacement parameters (\AA^2)

	U^{11}	U^{22}	U^{33}	U^{12}	U^{13}	U^{23}
O1	0.0627 (15)	0.0674 (16)	0.0241 (11)	0.0127 (14)	0.0039 (11)	0.0043 (11)
N1	0.0470 (15)	0.0298 (11)	0.0291 (12)	0.0001 (11)	0.0021 (11)	-0.0007 (10)
C1	0.0366 (15)	0.0449 (17)	0.0242 (14)	-0.0039 (13)	0.0001 (12)	-0.0004 (12)
O2	0.0439 (13)	0.0569 (15)	0.0272 (11)	0.0194 (11)	-0.0044 (10)	-0.0057 (10)
N2	0.0297 (13)	0.0499 (15)	0.0372 (14)	0.0040 (12)	0.0003 (11)	0.0029 (12)
C2	0.0494 (18)	0.0534 (19)	0.0330 (16)	0.0142 (16)	0.0088 (14)	-0.0023 (15)
O3	0.0459 (13)	0.0668 (16)	0.0357 (12)	0.0036 (12)	-0.0028 (10)	0.0172 (12)
C3	0.0517 (19)	0.0494 (18)	0.0355 (17)	0.0193 (17)	0.0019 (14)	0.0031 (15)
O4	0.0617 (17)	0.082 (2)	0.0356 (13)	0.0123 (16)	0.0113 (12)	0.0022 (14)
C4	0.0369 (15)	0.0426 (16)	0.0274 (14)	0.0044 (13)	-0.0007 (12)	0.0021 (12)
O5	0.0467 (13)	0.0819 (19)	0.0311 (11)	0.0097 (13)	0.0015 (10)	0.0159 (12)
C5	0.0261 (13)	0.0385 (15)	0.0281 (14)	-0.0001 (12)	0.0009 (11)	-0.0053 (12)
O6	0.0301 (11)	0.0578 (14)	0.0517 (14)	0.0071 (11)	0.0051 (10)	0.0140 (11)
C6	0.0318 (14)	0.0375 (15)	0.0294 (15)	0.0028 (12)	-0.0035 (12)	0.0009 (12)
O7	0.0643 (16)	0.0357 (11)	0.0382 (12)	-0.0033 (11)	0.0102 (11)	-0.0075 (10)
C7	0.0435 (16)	0.0425 (16)	0.0297 (14)	0.0083 (14)	0.0031 (13)	0.0020 (13)
O8	0.0834 (19)	0.0336 (11)	0.0347 (12)	-0.0046 (12)	0.0123 (12)	0.0041 (10)
C8	0.0374 (16)	0.0523 (18)	0.0295 (15)	0.0059 (14)	0.0017 (12)	0.0023 (14)
C9	0.0381 (16)	0.0403 (15)	0.0297 (15)	-0.0020 (13)	0.0008 (13)	0.0034 (13)

C10	0.0366 (16)	0.0436 (16)	0.0310 (15)	0.0000 (14)	0.0020 (12)	0.0030 (13)
C11	0.0376 (16)	0.0406 (16)	0.0315 (15)	-0.0057 (13)	-0.0039 (13)	0.0090 (13)
C12	0.0518 (19)	0.0478 (17)	0.0236 (14)	-0.0086 (16)	-0.0010 (13)	0.0062 (13)
C13	0.0485 (19)	0.0450 (17)	0.0324 (16)	-0.0022 (15)	0.0075 (14)	-0.0001 (13)
C14	0.0417 (16)	0.0448 (17)	0.0333 (15)	0.0014 (14)	0.0018 (13)	0.0040 (13)
C15	0.0305 (15)	0.0389 (15)	0.0294 (15)	0.0020 (13)	-0.0008 (12)	0.0029 (12)
C16	0.0323 (15)	0.0458 (17)	0.0354 (17)	0.0018 (13)	0.0001 (13)	0.0105 (14)
C17	0.058 (2)	0.103 (3)	0.0294 (17)	0.004 (2)	-0.0044 (16)	-0.002 (2)
C18	0.111 (5)	0.121 (5)	0.093 (4)	-0.052 (4)	0.023 (4)	-0.062 (4)
C19	0.054 (2)	0.063 (3)	0.083 (3)	-0.018 (2)	0.005 (2)	-0.003 (2)
C20	0.0404 (15)	0.0294 (13)	0.0280 (14)	-0.0022 (12)	0.0035 (12)	-0.0017 (11)
C21	0.078 (3)	0.053 (2)	0.043 (2)	-0.014 (2)	-0.0174 (19)	-0.0079 (17)
C22	0.073 (3)	0.089 (3)	0.088 (4)	-0.044 (3)	-0.027 (3)	0.008 (3)
C23	0.049 (2)	0.057 (2)	0.069 (3)	-0.0053 (18)	0.0188 (19)	0.012 (2)
C24	0.0420 (16)	0.0321 (14)	0.0309 (14)	-0.0060 (13)	0.0039 (13)	-0.0023 (12)

Geometric parameters (\AA , $^\circ$)

O1—C1	1.349 (4)	C8—H8	0.9300
O1—H1'	0.96 (6)	C9—C10	1.398 (5)
N1—C23	1.495 (5)	C9—C14	1.403 (5)
N1—C20	1.497 (4)	C10—C11	1.390 (4)
N1—H1A	0.8900	C10—H10	0.9300
N1—H1B	0.8900	C11—C12	1.383 (5)
C1—C2	1.387 (5)	C12—C13	1.391 (5)
C1—C6	1.397 (5)	C12—H12	0.9300
O2—C5	1.369 (4)	C13—C14	1.384 (4)
O2—H2'	0.82 (2)	C14—H14	0.9300
N2—C16	1.492 (4)	C15—C16	1.541 (4)
N2—C19	1.498 (5)	C16—C17	1.535 (5)
N2—H2A	0.8900	C16—H16	0.9800
N2—H2B	0.8900	C17—C18	1.497 (8)
C2—C3	1.380 (5)	C17—H17A	0.9700
C2—H2	0.9300	C17—H17B	0.9700
O3—C11	1.367 (4)	C18—C19	1.456 (8)
O3—H3'	0.87 (6)	C18—H18A	0.9700
C3—C4	1.398 (5)	C18—H18B	0.9700
C3—H3	0.9300	C19—H19A	0.9700
O4—C13	1.387 (4)	C19—H19B	0.9700
O4—H4'	0.89 (2)	C20—C24	1.526 (4)
C4—C5	1.400 (4)	C20—C21	1.531 (5)
C4—C7	1.464 (4)	C20—H20	0.9800
O5—C15	1.219 (4)	C21—C22	1.488 (7)
C5—C6	1.389 (4)	C21—H21A	0.9700
O6—C15	1.269 (4)	C21—H21B	0.9700
C6—H6	0.9300	C22—C23	1.485 (7)
O7—C24	1.234 (4)	C22—H22A	0.9700
C7—C8	1.320 (5)	C22—H22B	0.9700

C7—H7	0.9300	C23—H23A	0.9700
O8—C24	1.268 (4)	C23—H23B	0.9700
C8—C9	1.471 (4)		
C1—O1—H1'	109.5	C13—C14—H14	120.3
C23—N1—C20	107.4 (3)	C9—C14—H14	120.3
C23—N1—H1A	110.2	O5—C15—O6	127.2 (3)
C20—N1—H1A	110.2	O5—C15—C16	118.5 (3)
C23—N1—H1B	110.2	O6—C15—C16	114.3 (3)
C20—N1—H1B	110.2	N2—C16—C17	103.7 (3)
H1A—N1—H1B	108.5	N2—C16—C15	109.0 (3)
O1—C1—C2	122.9 (3)	C17—C16—C15	113.0 (3)
O1—C1—C6	117.4 (3)	N2—C16—H16	110.3
C2—C1—C6	119.8 (3)	C17—C16—H16	110.3
C5—O2—H2'	112 (3)	C15—C16—H16	110.3
C16—N2—C19	106.6 (3)	C18—C17—C16	104.1 (3)
C16—N2—H2A	110.4	C18—C17—H17A	110.9
C19—N2—H2A	110.4	C16—C17—H17A	110.9
C16—N2—H2B	110.4	C18—C17—H17B	110.9
C19—N2—H2B	110.4	C16—C17—H17B	110.9
H2A—N2—H2B	108.6	H17A—C17—H17B	109.0
C3—C2—C1	119.0 (3)	C19—C18—C17	109.8 (4)
C3—C2—H2	120.5	C19—C18—H18A	109.7
C1—C2—H2	120.5	C17—C18—H18A	109.7
C11—O3—H3'	109.5	C19—C18—H18B	109.7
C2—C3—C4	123.2 (3)	C17—C18—H18B	109.7
C2—C3—H3	118.4	H18A—C18—H18B	108.2
C4—C3—H3	118.4	C18—C19—N2	106.0 (4)
C13—O4—H4'	102 (3)	C18—C19—H19A	110.5
C3—C4—C5	116.5 (3)	N2—C19—H19A	110.5
C3—C4—C7	122.5 (3)	C18—C19—H19B	110.5
C5—C4—C7	121.0 (3)	N2—C19—H19B	110.5
O2—C5—C6	120.2 (3)	H19A—C19—H19B	108.7
O2—C5—C4	118.3 (3)	N1—C20—C24	110.8 (2)
C6—C5—C4	121.5 (3)	N1—C20—C21	104.7 (3)
C5—C6—C1	120.0 (3)	C24—C20—C21	111.9 (3)
C5—C6—H6	120.0	N1—C20—H20	109.7
C1—C6—H6	120.0	C24—C20—H20	109.7
C8—C7—C4	126.8 (3)	C21—C20—H20	109.7
C8—C7—H7	116.6	C22—C21—C20	106.8 (3)
C4—C7—H7	116.6	C22—C21—H21A	110.4
C7—C8—C9	126.4 (3)	C20—C21—H21A	110.4
C7—C8—H8	116.8	C22—C21—H21B	110.4
C9—C8—H8	116.8	C20—C21—H21B	110.4
C10—C9—C14	119.5 (3)	H21A—C21—H21B	108.6
C10—C9—C8	118.5 (3)	C23—C22—C21	107.6 (3)
C14—C9—C8	122.0 (3)	C23—C22—H22A	110.2
C11—C10—C9	120.0 (3)	C21—C22—H22A	110.2

C11—C10—H10	120.0	C23—C22—H22B	110.2
C9—C10—H10	120.0	C21—C22—H22B	110.2
O3—C11—C12	122.8 (3)	H22A—C22—H22B	108.5
O3—C11—C10	116.8 (3)	C22—C23—N1	103.7 (3)
C12—C11—C10	120.4 (3)	C22—C23—H23A	111.0
C11—C12—C13	119.6 (3)	N1—C23—H23A	111.0
C11—C12—H12	120.2	C22—C23—H23B	111.0
C13—C12—H12	120.2	N1—C23—H23B	111.0
C14—C13—O4	119.9 (3)	H23A—C23—H23B	109.0
C14—C13—C12	121.0 (3)	O7—C24—O8	125.8 (3)
O4—C13—C12	119.1 (3)	O7—C24—C20	120.3 (3)
C13—C14—C9	119.5 (3)	O8—C24—C20	113.8 (3)
O1—C1—C2—C3	−179.3 (4)	O4—C13—C14—C9	176.4 (3)
C6—C1—C2—C3	0.9 (5)	C12—C13—C14—C9	−2.3 (5)
C1—C2—C3—C4	−1.7 (6)	C10—C9—C14—C13	0.7 (5)
C2—C3—C4—C5	1.4 (6)	C8—C9—C14—C13	179.7 (3)
C2—C3—C4—C7	−178.2 (4)	C19—N2—C16—C17	−31.3 (4)
C3—C4—C5—O2	178.9 (3)	C19—N2—C16—C15	89.3 (3)
C7—C4—C5—O2	−1.5 (5)	O5—C15—C16—N2	−2.2 (4)
C3—C4—C5—C6	−0.4 (5)	O6—C15—C16—N2	179.3 (3)
C7—C4—C5—C6	179.3 (3)	O5—C15—C16—C17	112.5 (4)
O2—C5—C6—C1	−179.6 (3)	O6—C15—C16—C17	−66.0 (4)
C4—C5—C6—C1	−0.3 (5)	N2—C16—C17—C18	27.9 (5)
O1—C1—C6—C5	−179.7 (3)	C15—C16—C17—C18	−89.9 (5)
C2—C1—C6—C5	0.1 (5)	C16—C17—C18—C19	−14.9 (8)
C3—C4—C7—C8	−15.6 (6)	C17—C18—C19—N2	−4.2 (8)
C5—C4—C7—C8	164.8 (3)	C16—N2—C19—C18	22.5 (6)
C4—C7—C8—C9	−178.4 (3)	C23—N1—C20—C24	99.1 (3)
C7—C8—C9—C10	−179.2 (4)	C23—N1—C20—C21	−21.8 (4)
C7—C8—C9—C14	1.8 (6)	N1—C20—C21—C22	3.7 (5)
C14—C9—C10—C11	1.8 (5)	C24—C20—C21—C22	−116.5 (4)
C8—C9—C10—C11	−177.2 (3)	C20—C21—C22—C23	15.9 (6)
C9—C10—C11—O3	176.4 (3)	C21—C22—C23—N1	−29.0 (5)
C9—C10—C11—C12	−2.8 (5)	C20—N1—C23—C22	31.5 (4)
O3—C11—C12—C13	−178.0 (3)	N1—C20—C24—O7	−4.1 (4)
C10—C11—C12—C13	1.1 (5)	C21—C20—C24—O7	112.4 (4)
C11—C12—C13—C14	1.4 (5)	N1—C20—C24—O8	176.9 (3)
C11—C12—C13—O4	−177.3 (3)	C21—C20—C24—O8	−66.5 (4)

Hydrogen-bond geometry (Å, °)

D—H···A	D—H	H···A	D···A	D—H···A
O1—H1'···O8	0.96	1.70	2.642 (4)	169
O2—H2'···O6	0.82 (2)	1.83 (3)	2.647 (3)	175 (5)
O3—H3'···O2 ⁱ	0.87	1.92	2.784 (3)	171
O4—H4'···O7 ⁱⁱ	0.89 (2)	1.95 (3)	2.794 (4)	159 (4)
N1—H1B···O5 ⁱⁱⁱ	0.89	2.04	2.827 (3)	146

N1—H1A···O8 ^{iv}	0.89	1.90	2.733 (4)	154
N2—H2A···O4 ^v	0.89	2.11	2.920 (4)	150
N2—H2B···O6 ^{vi}	0.89	1.87	2.734 (4)	163
C6—H6···O6	0.93	2.61	3.282 (4)	130

Symmetry codes: (i) $-x, y+1/2, -z+1/2$; (ii) $x+1/2, -y+3/2, -z+1$; (iii) $-x+1/2, -y+1, z+1/2$; (iv) $-x, y-1/2, -z+3/2$; (v) $-x+1, y-1/2, -z+1/2$; (vi) $x+1/2, -y+1/2, -z+1$.